A Gyrification Analysis Approach Based on Laplace Beltrami Eigenfunction Level Sets

Supplementary Material

Rosita Shishegar[a,b,c,d], Fabrizio Pizzagalli[e,f], Nellie Georgiou-Karistianis[a], Gary F. Egan[a,b], Neda Jahanshad[e], Leigh A. Johnston[c,g]

[a]School of Psychological Sciences and Turner Institute for Brain and Mental Health, Monash University, Melbourne, Australia, [b]Monash Biomedical Imaging, Monash University, Melbourne, Australia, [c]Department of Biomedical Engineering, University of Melbourne, Melbourne, Australia, [d]The Australian e-Health Research Centre, CSIRO, Melbourne, Australia, [e]Imaging Genetics Center, Mark and Mary Stevens Neuroimaging and Informatics Institute, Keck School of Medicine of USC, University of Southern California, Los Angeles, CA, USA, [f]Department of Neurosciences, University of Turin, Italy, [g]Melbourne Brain Centre Imaging Unit, University of Melbourne, Melbourne, Australia.

Synthetic data analysis

We generated synthetic developing brain surfaces using a longitudinal growth model proposed by Wang et al. (2019). Wang et al. (2019) showed that both initial cortical thickness and time affect the folding patterns during development. We generated synthetic cortical surfaces at 34, 38 and 42 weeks of gestation from a sphere with initial cortical thickness 4.3 mm.

In order to compare the proposed gyrification method with Luders' GI and mean curvature, GI values were calculated on these simple synthetic surfaces of the brains. Given the smaller size of the generated synthetic brains compared to developing human brains, we adjusted the heat kernel filter in Luders' GI method to 8mm FWHM. This filter size was chosen in a trade-off to generate results similar to Luders et al. (2006, Figure 1) and to present minimal smoothing of the resultant gyral map. The LB-GI tuning parameter d_{thr} was also adjusted for the synthetic brains to 5mm. It was selected by manual quality checking of detected gyral and sulcal points along randomly selected level sets.

To further compare the LB-GI, Luders' GI, and mean curvature maps, pairwise correlations between the three metrices were calculated. An example of GI development over time for five different vertices is plotted in Figure S.3, with GI values on y-axis and gestational week on x-axis. Four vertices, P1-P4, were selected along the longest sulcal fundus on the synthetic brain at 42 weeks of gestation. Vertex P5 was selected on a second sulcal fundus. The corresponding vertices are selected on synthetic brains at 34 and 38 weeks of gestation.

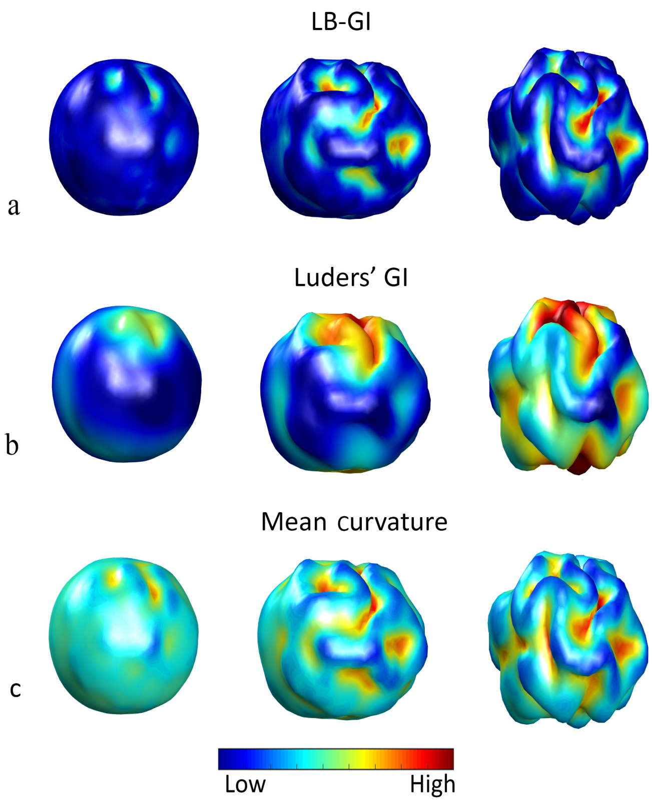

Figure S1. Comparison of GI values for synthetic developmental brain surfaces, showing (a) LB-GI, (b) Luders' GI, and (c) mean curvature maps. Simulations were performed using a longitudinal growth model of the cortical surface proposed by Wang et al. (2019) starting from a sphere with initial cortical thickness 4.3 mm. The GI values are colour coded on the simulation surfaces at gestational age 34 weeks (left), 38 weeks (middle) and 42 weeks (right)."

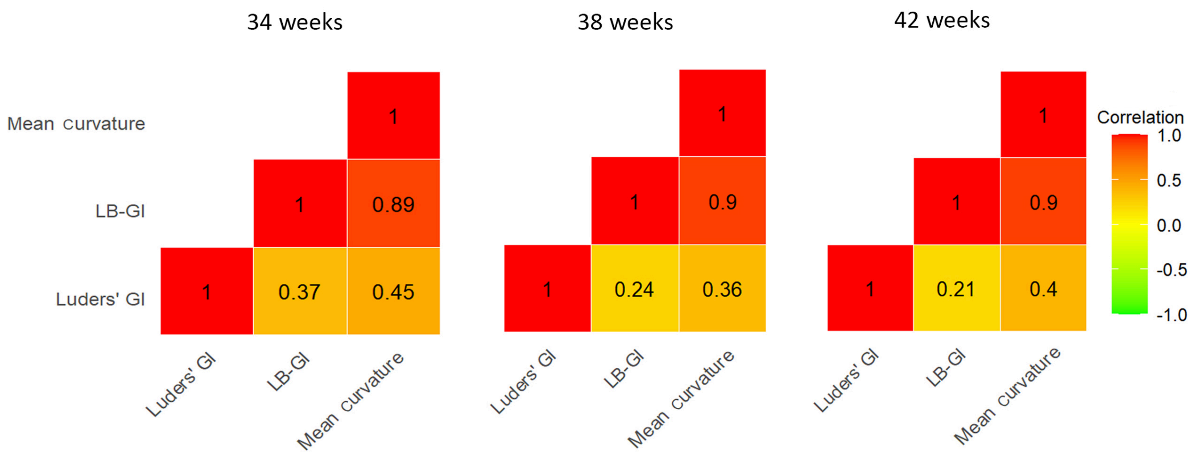

Figure S2. Correlation between LB-GI, Luders' GI and mean curvature maps calculated for synthetic brain surfaces at gestational ages 34, 38 and 42 weeks.

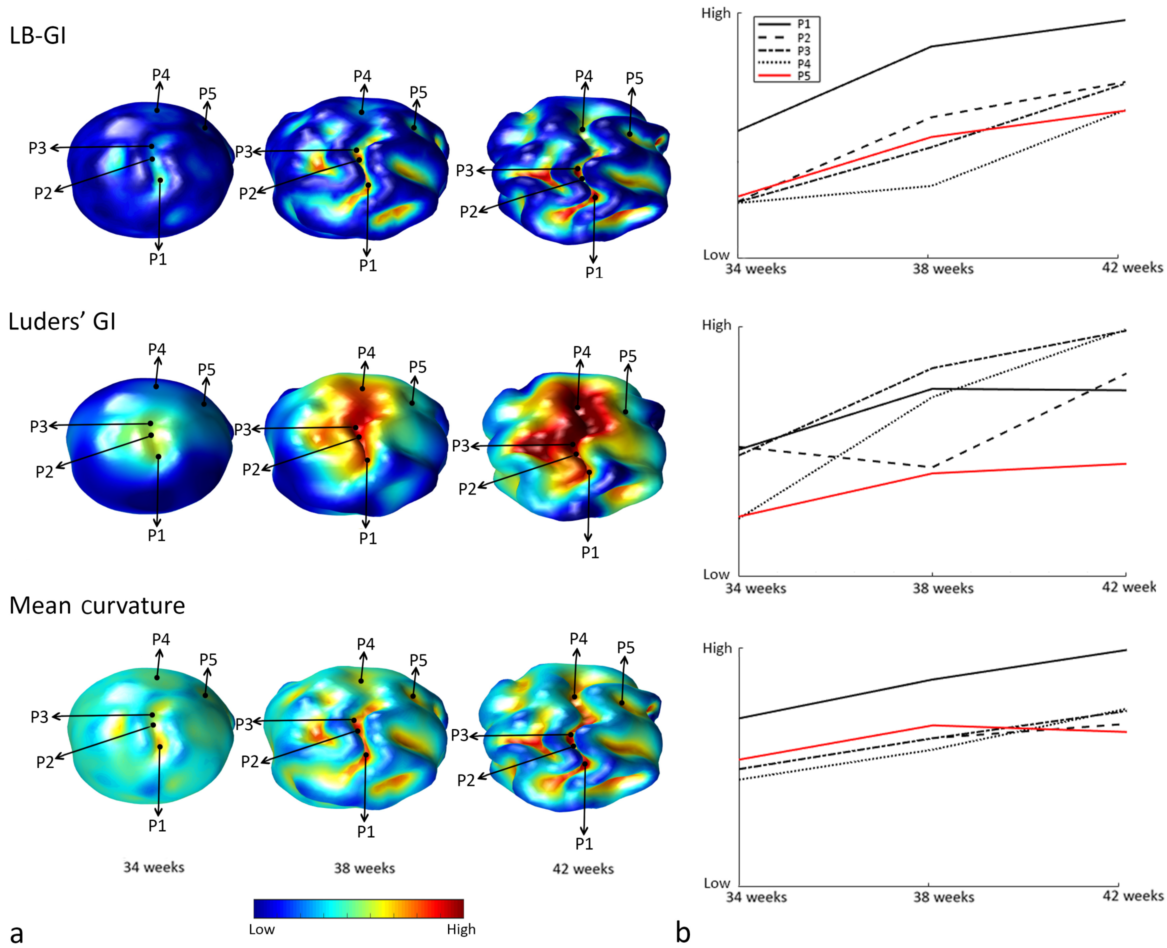

Figure S3. Longitudinal changes in gyrification for selected sulcal vertices calculated for synthetic brains at 34, 38 and 42 weeks of gestation. (a) LB-GI (top row), Luders' GI (middle row), and Mean curvature (bottom row) rendered on the superior view of the synthetic brains. The illustrated vertices P1-P4 lie along the longest sulcal fundus on the synthetic brain 42 weeks of gestation. Vertex P5 is situated on a neighbouring sulcal fundus. (b) GI values measured at vertices P1-P5 over gestational weeks 34, 38 and 42.

Results: Synthetic data

Figure S1 illustrates the LB-GI, Luders' GI and mean curvature maps color coded on the simple synthetic surfaces of the brains at gestational age 34, 38 and 42 weeks. The LB-GI represents both depth and curvature, resulting in the detection of more regional cortical folding differences along and between different sulci compared to the Luders' GI and mean curvature. The LB-GI map at 42 weeks surface demonstrates differences in the observable sulcal fundi, while the mean curvature map assigns very similar values in these sulci. Furthermore, LB-GI presents consistent assignment of minimal values to all gyral ridge points instead of only some sharply curved gyral point, as in mean curvature. Similar results were reported in our previous study of development using fetal sheep brains (Fig 3.13, Fig

4.8, Fig 4.9 and Fig 4.10; Shishegar 2017). Luders' GI captures the overall patterns of folding and shows the global regions with higher gyrification but not the detailed cortical folding patterns while these details are revealed by LB-GI method, especially in sulcal regions. Figure S2 presents the pairwise correlation between LB-GI, Luders' GI and mean curvature maps calculated for synthetic brain surfaces at gestational age 34, 38 and 42 weeks. As visualised in Figure S1, LB-GI is more closely associated with mean curvature than Luders' GI.

An example of longitudinal changes in gyrification is presented on Figure S3 over five selected sulcal vertices. In comparison with Luders' GI and mean curvature, the LB-GI tracks age-related brain development more accurately by demonstrating the expected increase in the gyrification. This increase in LB-GI is observed for all vertices P1-P4, (Fig. S3, black lines), and P5 (Fig.S3, red lines), whereas for Luders' GI and mean curvature, not all vertices demonstrated monotonic increase in GI value during development of these sulci.

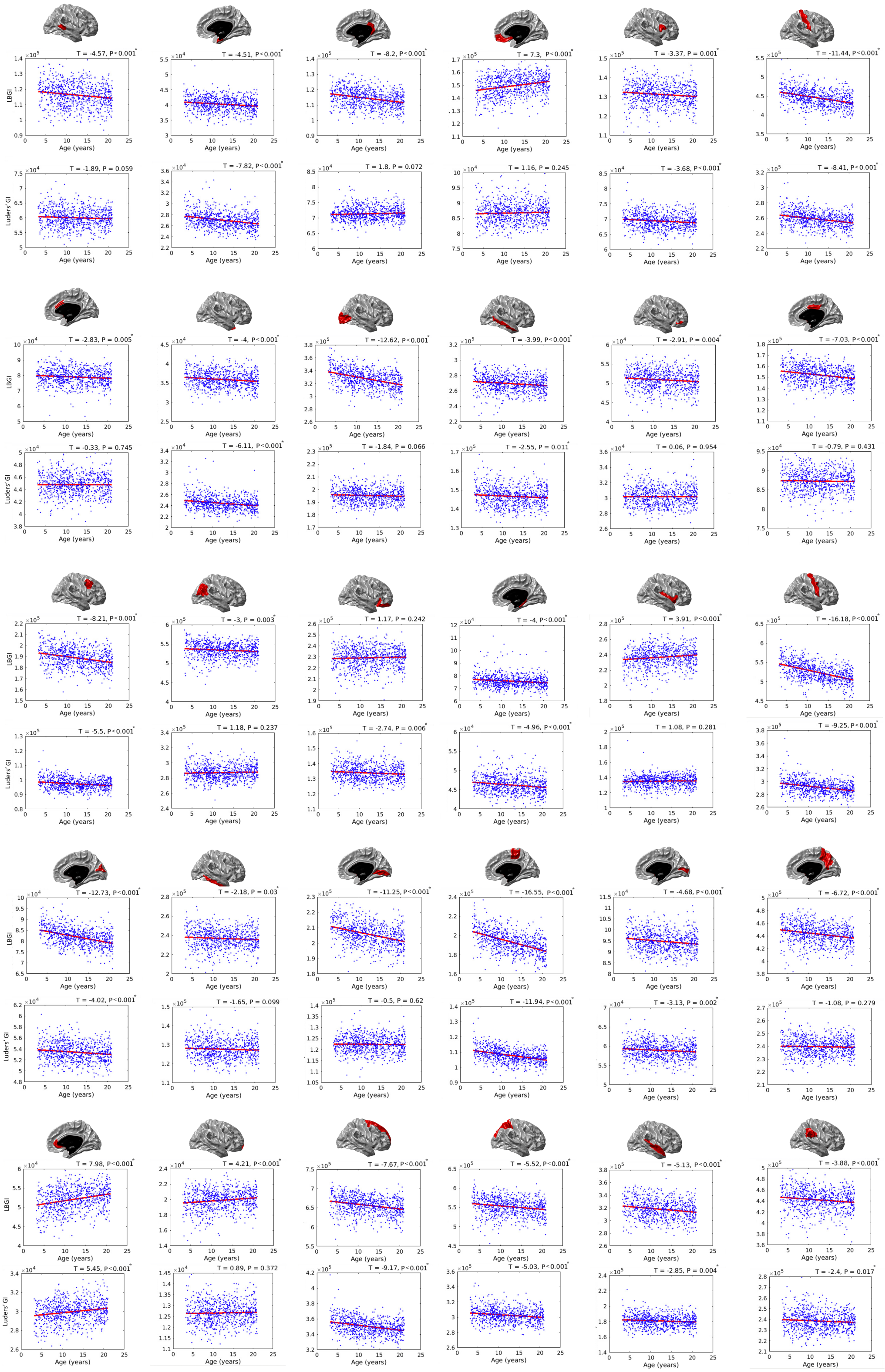
LBGI
Luders' GI
Age (years)
T = -4.57, P<0.001*
T = -4.51, P<0.001*
T = -8.2, P<0.001*
T = 7.3, P<0.001*
T = -3.37, P = 0.001*
T = -11.44, P<0.001*
T = -1.89, P = 0.059
T = -7.82, P<0.001*
T = 1.8, P = 0.072
T = 1.16, P = 0.245
T = -3.68, P<0.001*
T = -8.41, P<0.001*
T = -2.83, P = 0.005*
T = -4, P<0.001*
T = -12.62, P<0.001*
T = -3.99, P<0.001*
T = -2.91, P = 0.004*
T = -7.03, P<0.001*
T = -0.33, P = 0.745
T = -6.11, P<0.001*
T = -1.84, P = 0.066
T = -2.55, P = 0.011*
T = 0.06, P = 0.954
T = -0.79, P = 0.431
T = -8.21, P<0.001*
T = -3, P = 0.003*
T = 1.17, P = 0.242
T = -4, P<0.001*
T = 3.91, P<0.001*
T = -16.18, P<0.001*
T = -5.5, P<0.001*
T = 1.18, P = 0.237
T = -2.74, P = 0.006*
T = -4.96, P<0.001*
T = 1.08, P = 0.281
T = -9.25, P<0.001*
T = -12.73, P<0.001*
T = -2.18, P = 0.03*
T = -11.25, P<0.001*
T = -16.55, P<0.001*
T = -4.68, P<0.001*
T = -6.72, P<0.001*
T = -4.02, P<0.001*
T = -1.65, P = 0.099
T = -0.5, P = 0.62
T = -11.94, P<0.001*
T = -3.13, P = 0.002*
T = -1.08, P = 0.279
T = 7.98, P<0.001*
T = 4.21, P<0.001*
T = -7.67, P<0.001*
T = -5.52, P<0.001*
T = -5.13, P<0.001*
T = -3.88, P<0.001*
T = 5.45, P<0.001*
T = 0.89, P = 0.372
T = -9.17, P<0.001*
T = -5.03, P<0.001*
T = -2.85, P = 0.004*
T = -2.4, P = 0.017*

Figure S4. Association between age and average gyrification values across all vertices within the gyral-based parcellations extracted by FreeSurfer based on the anatomical Desikan-Killiany atlas. Each cortical parcellation is red on the lateral/medial view of right hemisphere of an averaged atlas. The upper panels show the LB-GI values of the parcellation as a function of age. The lower panels show the values of Luders' GI of the parcellation as a function of age. The values are adjusted for gender. T-statistics and *p*-values (**p*<0.05) are reported.